Electronic Supplementary Material (ESI) for Sustainable Energy & Fuels.
This journal is © The Royal Society of Chemistry 2021

Supporting Information

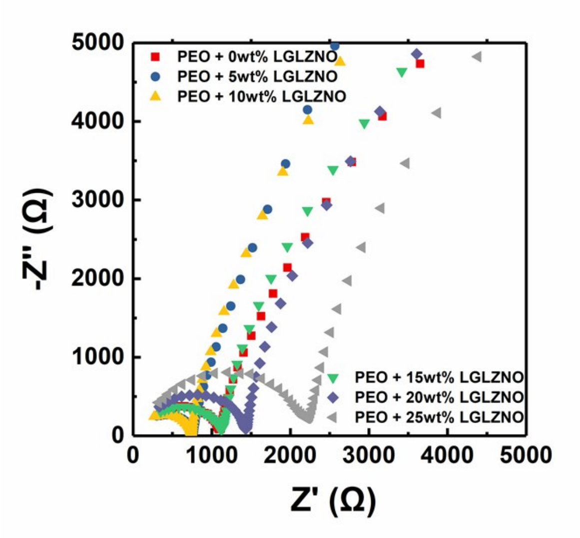

Figure S1. Nyquist plots of the composite electrolytes with changed LGLZNO contents in PEO under 30 ℃.

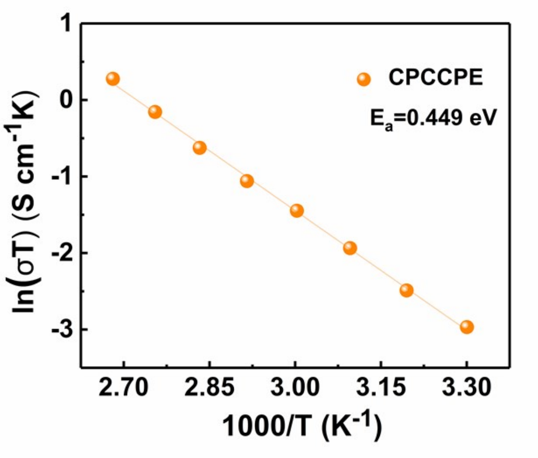

Figure S2. Ionic conductivity of CPCCPE versus temperature and corresponding activation energy (E_a).

The E_a of CPCCPE can be obtained from the equation S1:

$$\sigma T = A\exp\left(\frac{-E_a}{k_B T}\right)$$

S1

Where σ is the conductivity, T is the absolute temperature, A and k_B are the pre-exponential parameter, Boltzmann's constant.

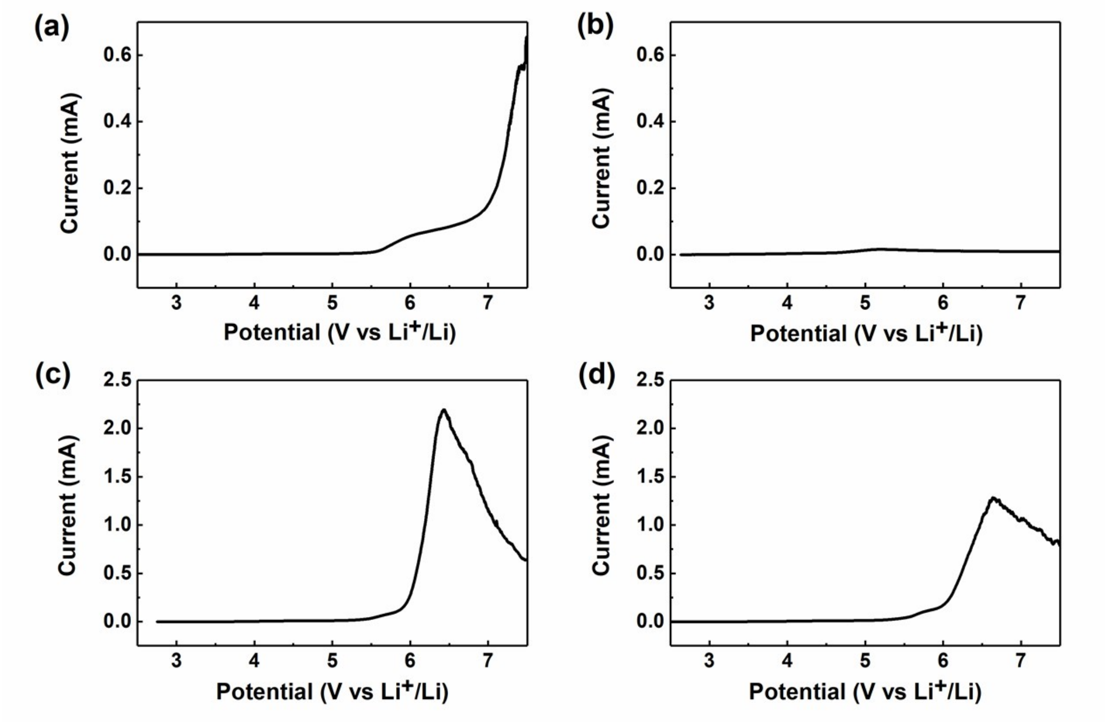

Figure S3. The LSV curves with different compositions at 60 °C. (a) Li/LGLZNO+PEO/stainless steel, LGLZNO+PEO represents the LGLZNO electrolytes with both sides coated by PEO; (b) Li/LGLZNO/stainless steel, (c) Li/PEO/stainless steel and (d) Li/composite electrolyte/stainless steel, the composite electrolyte means the 10 wt.% LGLZNO powder dispersed into PEO matrix.

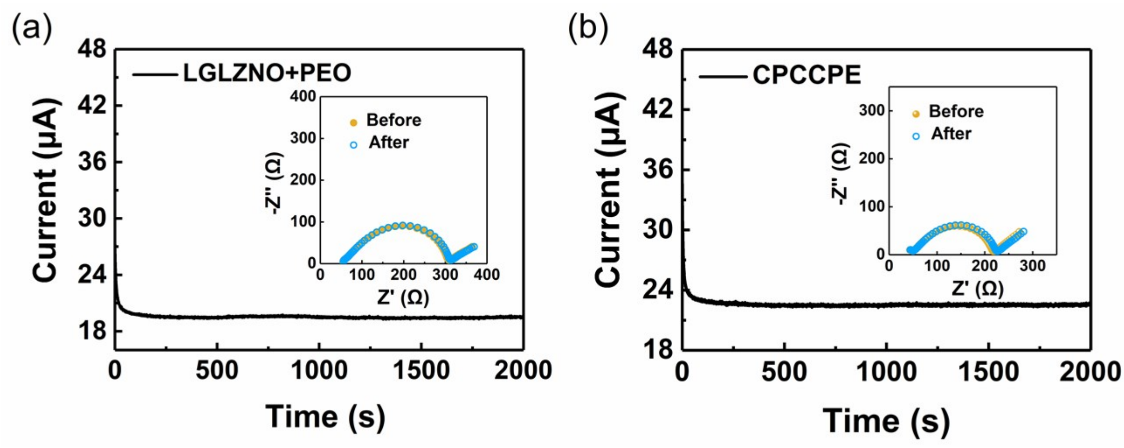

Figure S4. The chronoamperometry curves and the corresponding Nyquist plots (insert figures) before and after polarization for Li/Li symmetrical batteries of (a) LGLZNO and (b) CPCCPE.

The Li ions transfer number (t_{Li^+}) can be obtained from the equation S1:

$$t_{Li^+} = \frac{I_s(\Delta V - I_0 R_0)}{I_0(\Delta V - I_s R_s)} \quad \text{S2}$$

Where ΔV is the polarization potential (10 mV), I_0 and R_0 are the initial current and resistance, and I_s and R_s are the steady-state current and resistance.

Table S1. The Li-ion transference number (t_{Li^+}) of LGLZNO+PEO and CPCCPE at 60 °C.

Samples	I_0(μA)	I_s(μA)	R_0(ohm)	R_s(ohm)	ΔV(mV)	t_{Li+}
LGLZNO+PEO	27.79	19.46	308.5	313.5	10	0.256
CPCCPE	35.85	22.58	217	225	10	0.284

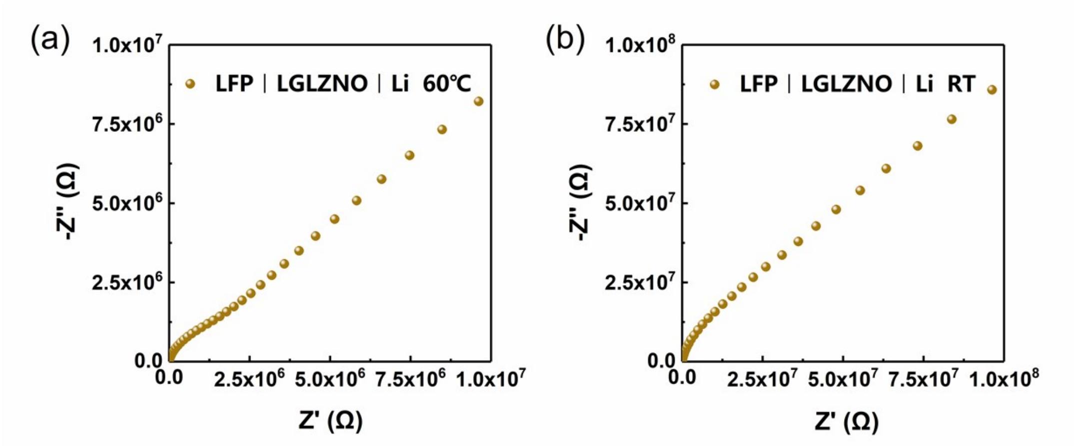

Figure S5. (a, b) Nyquist plots of LFP/LGLZNO/Li full cells at 60 ℃ and LFP/GLZNO/Li full cells at RT.

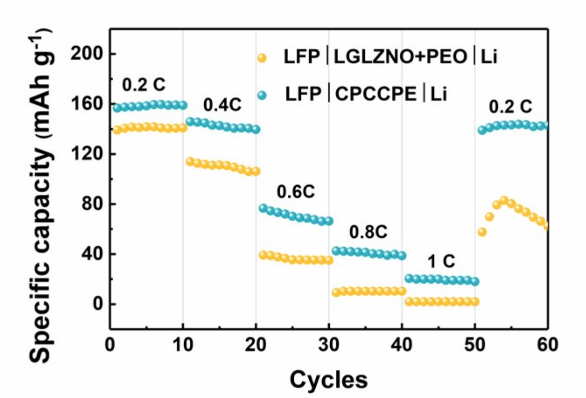

Figure S6. Rate performances at 60 ℃ of LFP/LGLZNO+PEO/Li and LFP/CPCCPE/Li full cells.

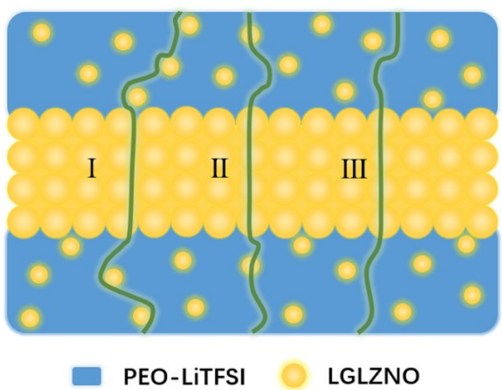

Figure S7. Three possible pathways for Li-ions transportation in CPCCPE.

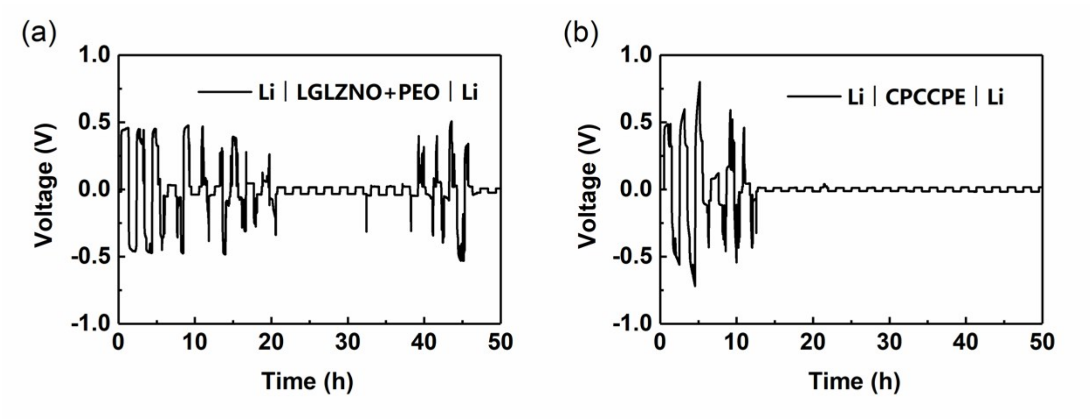

Figure S8. (a, b) Voltage profiles of the lithium plating/stripping cycling of Li/LGLZNO+PEO/Li and Li/CPCCPE/Li with a current density of 100 μA cm^{-2} at RT.

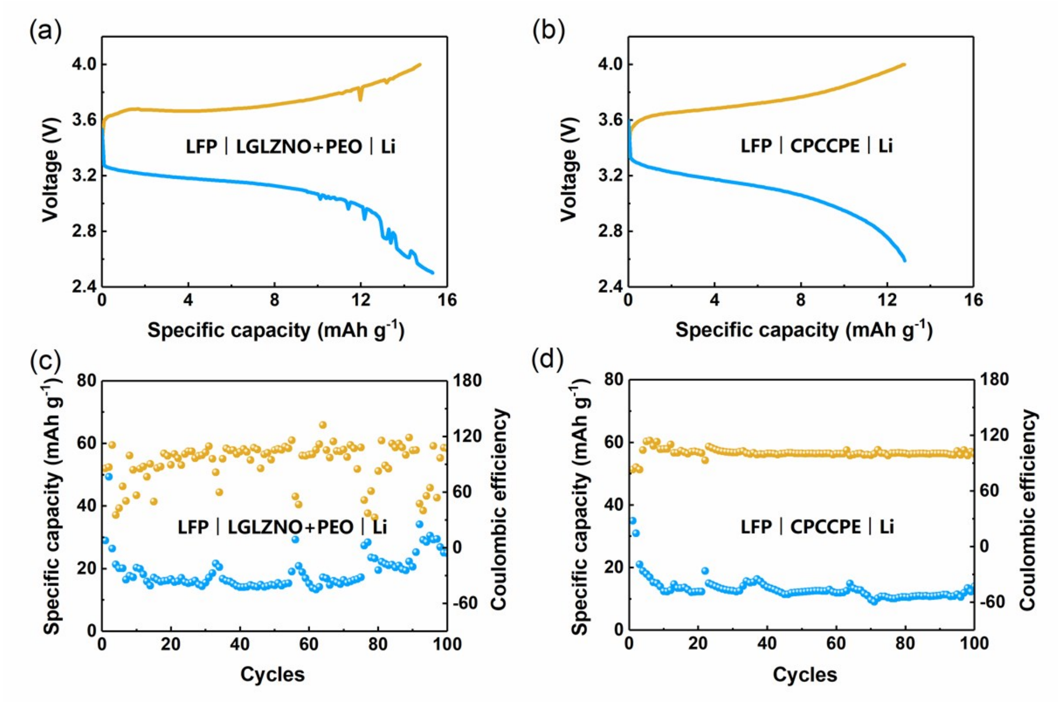

Figure S9. (a, b) Charge/discharge voltage profiles of the 15th cycle at 0.2 C and RT for LFP/LGLZNO+PEO/Li and LFP/CPCCPE/Li full cells. (c, d) Cycling performance of LFP/ LGLZNO+PEO/Li and LFP/CPCCPE/Li full cells at 0.2 C and RT.

Table S2. Performance comparison of polymer and inorganic ceramic as composite electrolyte in full cells with LFP as cathode material. (Note: "+" means to mix two or three together and "/" means that different electrolyte layers are superimposed together).

Solid electrolyte	Specific Test parameters	capacity after 100 cycles (mAh g^{-1})	Coulomb efficiency (%)	Maximum capacity retention after 100 cycles (%)	Ref.
PEO/LLZTO	90 °C 0.2 C	≈136	≈99.6	≈95	[1]
PCPSE/LATP	65 °C 0.2 C	130	97-100	≈95.5	[2]
PEO+LLZTO	60 °C 1 C	140	>99	≈100	[3]
PEO+PVDF+LGLZBO	60 °C 0.1 C	128.3	≈100	≈96.5	[4]
PEO+LLZO	55 °C 0.2 C	≈151.5	>99.8	≈94.5	[5]
PVDF+LLZTO	55 °C 0.2 C	≈143	≈99.6	94.7	[6]
PEO+LGLZNO/LGLZNO	60 °C 0.2 C	158	≈99.8	≈100	This work

References

[1] S.-S. Chi; Y. Liu; N. Zhao; X. Guo; C.-W. Nan; L.-Z. Fan, Solid polymer electrolyte soft interface layer with 3D lithium anode for all-solid-state lithium batteries, Energy Storage Mater. 17 (2019) 309-316.

[2] W. Zhou; S. Wang; Y. Li; S. Xin; A. Manthiram; J. B. Goodenough, Plating a Dendrite-Free Lithium Anode with a Polymer/Ceramic/Polymer Sandwich Electrolyte, J. Am. Chem. Soc. 138 (2016) 9385-9388.

[3] T. Thompson; S. Yu; L. Williams; R. D. Schmidt; R. Garcia-Mendez; J. Wolfenstine; J. L. Allen; E. Kioupakis; D. J. Siegel; J. Sakamoto, Electrochemical Window of the Li-Ion Solid Electrolyte $Li_7La_3Zr_2O_{12}$, ACS Energy Lett. 2 (2017) 462-468.

[4] J. Li; K. Zhu; Z. Yao; G. Qian; J. Zhang; K. Yan; J. Wang, A promising composite solid electrolyte incorporating LLZO into PEO/PVDF matrix for all-solid-state lithium-ion batteries, Ionics 26 (2019) 1101-1108.

[5] H. Duan; Y.-X. Yin; Y. Shi; P.-F. Wang; X.-D. Zhang; C.-P. Yang; J.-L. Shi; R. Wen; Y.-G. Guo; L.-J. Wan, Dendrite-Free Li-Metal Battery Enabled by a Thin Asymmetric Solid Electrolyte with Engineered Layers, J. Am. Chem. Soc. 140 (2017) 82-85.

[6] J. Lu; Y. Liu; P. Yao; Z. Ding; Q. Tang; J. Wu; Z. Ye; K. Huang; X. Liu, Hybridizing poly(vinylidene fluoride-co-hexafluoropropylene) with $Li_{6.5}La_3Zr_{1.5}Ta_{0.5}O_{12}$ as a lithium-ion electrolyte for solid state lithium metal batteries, Chem. Eng. J. 367 (2019) 230-238.